

FLOW AT THE VERTEX OF A WEDGE NEAR THE CONDITION
OF SHOCK DETACHMENT

by Jerry C. South, Jr.
N.A.S.A., Langley Research Center

SUMMARY

The process of transition to shock-wave detachment for a finite wedge in a uniform stream is reexamined. An asymptotic analysis in a transformed physical plane yields closed-form solutions valid in a neighborhood of the wedge vertex. The transformed coordinates facilitate the application of boundary conditions, and should be useful in the analogous problem for a cone. Quantitative results are obtained which verify the conclusions of Guderley's hodograph analysis.

FACILITY FORM 802	N66.87607	
	(ACCESSION NUMBER)	(THRU)
	25	<i>None</i>
	(PAGES)	(CODE)
	TMX 57997	
	(NASA CR OR TMX OR AD NUMBER)	(CATEGORY)

1. INTRODUCTION

In the classical solution for an infinite wedge placed in a steady, supersonic, uniform stream, it is well known that for sufficiently small wedge vertex angles θ , a straight oblique shock wave is attached at the vertex. The flow properties are constant between the shock wave and the wedge surface, and are determined by the jump conditions across the shock and flow tangency at the surface.

For given conditions in the uniform stream ahead of the wedge, there is a maximum vertex angle, θ_d , beyond which the shock wave is detached from the vertex, and the simple solution no longer exists. For all but a limited range of wedge angles smaller than θ_d , the flow in the "shock layer" is supersonic; however, there exists a vertex angle θ_s , $\theta_s < \theta_d$, such that the flow in the shock layer is sonic, and attached-shock, subsonic flow occurs in the range of angles $\theta_s < \theta < \theta_d$.

In a practical problem the wedge is, of course, finite in its extent downstream, and the classical infinite wedge solution is not valid in the large. In the range $\theta_s < \theta < \theta_d$, where the shock-layer flow is subsonic, the governing gas dynamic equations are of elliptic type; a change in the downstream boundary condition, expressing a departure from the straight wedge contour, can influence the entire solution. In this case, the classical solution occurs only at the vertex, while the shock wave is generally curved and the flow properties are not constant away from the tip.

Guderley (1947) studied the finite wedge, where he formulated a boundary problem for a simplified form of Chaplygin's equation for the stream function in the hodograph (velocity) plane. In his analysis, he discussed qualitatively the process of transition from attached-shock, supersonic flow to detached-shock, mixed (subsonic-supersonic) flow. In particular, he clarified the significance of "Crocco's point," a certain point on the shock polar diagram which corresponds to a change in sign of the streamline curvature behind a curved shock wave (Ferri, 1954). The wedge angle corresponding to Crocco's point, θ_c , lies within the subsonic-flow range, $\theta_s < \theta_c < \theta_d$; the indication of violent changes in the flow at this point caused Crocco (1937) to suspect that the shock detachment occurred there rather than at the larger wedge angle, θ_d . Guderley's analysis showed the conjecture to be false. He demonstrated that as the wedge angle is increased from θ_s to θ_d , the shock curvature at the vertex is zero for $\theta < \theta_c$; then nonzero, but finite, at $\theta = \theta_c$; and finally infinite, but still attached, for $\theta_c < \theta < \theta_d$.

A phenomenon similar to the Crocco-point behavior occurs in the classical solution for supersonic axisymmetric flow past a circular cone, but the governing equations preclude a closed-form analysis (Shen & Lin, 1951). In the basic infinite-cone problem, the shock wave is itself a conical surface with vertex at the cone tip, and flow properties are constant along any intermediate conical surface; but the solution can be obtained only by numerical integration of a nonlinear, two-point boundary problem (Kopal, 1947). The final analysis of detachment transition is

not amenable to treatment in the hodograph plane; analysis in the physical plane, or a minor transformation thereof, will likely be more straightforward. An asymptotic expansion at the cone vertex seems promising, and has already been used to obtain the ratio of the shock-wave and body curvatures at the tip of an ogive of revolution (Shen & Lin, 1951; Cabannes, 1951).

The present paper demonstrates that analysis of the wedge problem can be carried out in the physical plane in a straightforward manner with quantitative results; that Guderley's conclusions can be reached without resort to the hodograph treatment. An interesting and tractable eigenvalue problem is formulated whose closed-form solution offers a detailed picture of the behavior of the flow near the wedge vertex as transition to shock detachment occurs. The asymptotic technique which is used should be equally applicable to conical flow, with the expectation that closed-form solutions will not result because of the complexity of the basic infinite-cone solution

2. ANALYSIS

The flow geometry and coordinates are illustrated in figure 1. A body-oriented coordinate system is used with the x and y coordinates along and normal to the wedge surface, and with origin at the vertex. The basic equations are as follows:

$$\text{Continuity} \quad \frac{\partial}{\partial x} (\rho u) + \frac{\partial}{\partial y} (\rho v) = 0 \quad (1)$$

$$\text{x-momentum} \quad u \frac{\partial u}{\partial x} + v \frac{\partial u}{\partial y} + \frac{1}{\rho} \frac{\partial p}{\partial x} = 0 \quad (2)$$

$$\text{y-momentum} \quad u \frac{\partial v}{\partial x} + v \frac{\partial v}{\partial y} + \frac{1}{\rho} \frac{\partial p}{\partial y} = 0 \quad (3)$$

$$\text{Bernoulli} \quad \frac{2\gamma}{\gamma - 1} \frac{p}{\rho} + u^2 + v^2 = \text{constant} \quad (4)$$

The four unknown functions in equations (1) to (4) are u and v , the x and y components of velocity; and p and ρ , the static pressure and density. γ is the ratio of specific heats of the gas.

We will seek a local solution valid in a neighborhood of the wedge vertex such that along the shock wave, $y = \delta(x)$, the usual shock-wave relations (e.g., see South, 1964) are satisfied, and along the wedge surface, $y = 0$, the y -component of velocity vanishes; that is, $v(x, 0) = 0$.

Transformation of coordinates

To study the flow in a neighborhood of the wedge vertex, it is convenient to introduce a transformation which maps the shock layer into an open rectangular region. The coordinates ξ and η are introduced so that

$$\xi = x, \quad \eta = y/\delta(x) \quad (5)$$

where

$$\frac{d\delta}{dx} = \tan \lambda \quad (6)$$

and $\lambda = \beta - \theta$, the angle between the tangent to the shock wave and the wedge surface. Then the shock wave corresponds to the line $\eta = 1$ and

the wedge surface is the ξ -axis, $\eta = 0$ (fig. 2). Whereas in the original coordinates, the flow at the wedge vertex occurs at the point $x = 0$, $y = 0$, it is now "stretched out" along the η -axis, $\xi = 0$, $0 \leq \eta \leq 1$. After eliminating derivatives of ρ from equation (1) by using equations (2) to (4), the transformation of equations (1) to (3) yields

$$\delta \left(\frac{\partial u}{\partial \xi} + \frac{u}{\gamma p} \frac{\partial p}{\partial \xi} \right) + (v - u \eta \tan \lambda) \frac{1}{\gamma p} \frac{\partial p}{\partial \eta} - \eta \tan \lambda \frac{\partial u}{\partial \eta} + \frac{\partial v}{\partial \eta} = 0 \quad (7)$$

$$\delta \left(u \frac{\partial u}{\partial \xi} + \frac{1}{\rho} \frac{\partial p}{\partial \xi} \right) + (v - u \eta \tan \lambda) \frac{\partial u}{\partial \eta} - \eta \frac{\tan \lambda}{\rho} \frac{\partial p}{\partial \eta} = 0 \quad (8)$$

$$\delta u \frac{\partial v}{\partial \xi} + (v - u \eta \tan \lambda) \frac{\partial v}{\partial \eta} + \frac{1}{\rho} \frac{\partial p}{\partial \eta} = 0 \quad (9)$$

The boundary conditions are

$$v(\xi, 0) = 0 \quad (10)$$

and

$$f(\xi, 1) = F[\beta(\xi), \theta, \gamma, M_\infty] \quad (11)$$

where f represents any of the unknown functions u , v , p , or ρ , and the particular form for F is given by the usual shock-wave relations. M_∞ is the stream Mach number ahead of the wedge.

Asymptotic expansions

From physical considerations we expect a solution which coincides with the infinite-wedge solution at the vertex, $\xi = 0$; and such that the flow variables in a neighborhood of the tip are continuous, but may have infinite derivatives. Preliminary study of the equations (6) to (8), together with the condition that the shock is attached at the vertex, $\delta(0) = 0$, leads us to an asymptotic expansion for the unknown functions of the form

$$f(\xi, \eta) \sim f_0(\eta) + f_1(\eta)\xi^\alpha \quad (12)$$

where the exponent α is positive. (The symbol \sim will be used to denote equality to the lowest order in ξ indicated.) That form of solution is indeed found to be compatible with equations (7) to (8), with

$$\delta(\xi) \sim \xi \tan \lambda_0 \quad (13)$$

After substitution of the expansions (12) and (13) into equations (7) to (8) and equating coefficients of like powers of ξ , it can be verified that the zeroth-order functions $f_0(\eta)$ comprise the classical infinite-wedge solution, provided that $\alpha > 0$. It should be emphasized that the functions $f_0(\eta)$ are constant functions, where

$$f_0(\eta) = r(0, \eta) \equiv F[\beta(0), \theta, \gamma, M_\infty] = F_0 \quad (14)$$

and in particular

$$v_0(\eta) = v(0, \eta) \equiv 0 \quad (15)$$

The first-order functions $f_1(\eta)$ are found to satisfy the following system, where primes denote differentiation with respect to η :

$$\frac{u_0}{\gamma p_0} \tan \lambda_0 (\alpha p_1 - \eta p_1') + \tan \lambda_0 (\alpha u_1 - \eta u_1') + v_1' = 0 \quad (16)$$

$$\frac{\tan \lambda_0}{\rho_0} (\alpha p_1 - \eta p_1') + u_0 \tan \lambda_0 (\alpha u_1 - \eta u_1') = 0 \quad (17)$$

$$\frac{1}{\rho_0} p_1' + u_0 \tan \lambda_0 (\alpha v_1 - \eta v_1') = 0 \quad (18)$$

It is seen that the exponent α enters into the system as a parameter; later it will become clear that in the subsonic-flow range of vertex angles, $\theta_s < \theta < \theta_d$, α is an eigenvalue uniquely determined by the uniform stream conditions and the vertex angle θ . To satisfy the boundary conditions at the shock wave, equation (11), it is necessary that

$$\beta \sim \beta_0 + B_1 \xi^\alpha \quad (19)$$

and from equations (11) and (14),

$$\begin{aligned} f(\xi, 1) &\sim f(0, 1) + \frac{\partial F_0}{\partial \beta} (\beta - \beta_0) \\ &\sim f_0 + \frac{\partial F_0}{\partial \beta} B_1 \xi^\alpha \end{aligned} \quad (20)$$

Then the boundary conditions for equations (16) to (18) are

$$v_1(0) = 0 \quad (21)$$

and

$$f_1(1) = \frac{\partial F_0}{\partial \beta} B_1 \quad (22)$$

where, as mentioned before, f_1 represents any of the functions u_1 , v_1 , etc., and $\partial F_0 / \partial \beta$ is the corresponding β -derivative of the expression for the zeroth-order function at the shock wave (cf. eq. (14)).

Solution

The term $(\alpha u_1 - \eta v_1')$ is easily eliminated by combining equations (16) and (17) to yield

$$(1 - M_0^2) \tan \lambda_0 (\alpha p_1 - \eta p_1') - \rho_0 u_0 v_1' = 0 \quad (23)$$

where M_0 is the flow Mach number at the wedge vertex, $u_0 / \sqrt{\frac{\gamma p_0}{\rho_0}}$. If equations (18) and (23) are differentiated once again with respect to η , the function p_1 and its derivatives can be eliminated, with the result

$$(1 + C_0^2 \eta^2) v_1'' - 2(\alpha - 1) \overset{C_0^2}{\eta} v_1' + \alpha(\alpha - 1) C_0^2 v_1 = 0 \quad (24)$$

where

$$C_0^2 = (1 - M_0^2) \tan^2 \lambda_0 \quad (25)$$

It should be noted that in the subsonic-flow range of wedge angles, $\theta_s < \theta < \theta_d$, $M_0 < 1$, and C_0 is real; whereas in the supersonic range, $0 < \theta < \theta_s$, $M_0 > 1$, and C_0 is pure imaginary. The case $C_0 = 0$, where $M_0 = 1$, will be treated separately.

For $C_0 \neq 0$, equation (24) is simplified by the substitution $\xi = C_0 \eta$. Then,

$$(1 + \xi^2) \frac{d^2 v_1}{d\xi^2} - 2(\alpha - 1)\xi \frac{dv_1}{d\xi} + \alpha(\alpha - 1)v_1 = 0 \quad (26)$$

The boundary conditions in terms of the new independent variable ξ are:

$$\text{at } \xi = 0, \quad v_1 = 0 \quad (27)$$

$$\text{at } \xi = C_0 \text{ (i.e., } \eta = 1) \quad v_1 = \frac{\partial V_0}{\partial \beta} B_1 \quad (28)$$

Equation (26) is recognized to be a hypergeometric equation whose general solution can be written in terms of elementary functions:

$$v_1 = Ag(\xi) + Bh(\xi) \quad (29)$$

where

$$g(\xi) = (1 + i\xi)^\alpha - (1 - i\xi)^\alpha \quad (30a)$$

$$h(\xi) = (1 + i\xi)^\alpha + (1 - i\xi)^\alpha \quad (30b)$$

and A and B are arbitrary constants.

The variable ζ is either real or pure imaginary depending on whether $M_0 < 1$ or $M_0 > 1$, respectively. In the latter (supersonic shock-layer) case, both functions $g(\zeta)$ and $h(\zeta)$ are real-valued; and when $M_0 < 1$, $h(\zeta)$ is again real while $g(\zeta)$ is pure imaginary. In either case, the general solution (29) is, of course, real-valued. A convenient form for $g(\zeta)$ and $h(\zeta)$ when $M_0 < 1$ is:

$$g(\zeta) = 2i(1 + \zeta^2)^{\alpha/2} \sin \alpha\phi \quad (31a)$$

$$h(\zeta) = 2(1 + \zeta^2)^{\alpha/2} \cos \alpha\phi \quad (31b)$$

where

$$\phi = \tan^{-1} \zeta \quad (32)$$

Application of the boundary conditions (27) and (28) yields the final result

$$v_1 = \frac{\partial v_0}{\partial \beta} B_1 \frac{g(\zeta)}{g(C_0)} \quad (33)$$

or in terms of the original variable η ,

$$v_1(\eta) = \frac{\partial v_0}{\partial \beta} B_1 \frac{G(\eta)}{G(1)} \quad (34)$$

where

$$G(\eta) = g(C_0\eta) = (1 + iC_0\eta)^\alpha - (1 - iC_0\eta)^\alpha \quad (35)$$

Substitution of equation (34) into equation (18), integration, and application of boundary condition (22) then gives

$$p_1(\eta) = \left[c_1 - \rho_0 u_0 \tan \lambda_0 \frac{\partial v_0}{\partial \beta} \frac{H(\eta)}{i c_0 G(1)} \right] B_1 \quad (36)$$

where

$$H(\eta) = h(c_0 \eta) = (1 + i c_0 \eta)^\alpha + (1 - i c_0 \eta)^\alpha \quad (37)$$

and

$$c_1 = \frac{\partial p_0}{\partial \beta} + \rho_0 u_0 \tan \lambda_0 \frac{\partial v_0}{\partial \beta} \frac{H(1)}{i c_0 G(1)} \quad (38)$$

It will be seen later that the term c_1 is of special importance to the eigenvalue problem.

If $\alpha p_1 - \eta p_1'$ is now eliminated between equations (23) and (17), a differential equation for u_1 is obtained in terms of the known function v_1' . Then substitution of equation (34), integration, and application of the boundary condition (22) yields

$$u_1(\eta) = \left[c_2 \eta^\alpha + \tan \lambda_0 \frac{\partial v_0}{\partial \beta} \frac{H(\eta)}{i c_0 G(1)} \right] B_1 \quad (39)$$

where

$$c_2 = \frac{\partial u_0}{\partial \beta} - \tan \lambda_0 \frac{\partial v_0}{\partial \beta} \frac{H(1)}{i c_0 G(1)} \quad (40)$$

The solution for $\rho_1(\eta)$ can be obtained directly from the appropriate expansion of the Bernoulli equation (4), hence

$$\rho_1(\eta) = \rho_0 \left[\frac{p_1(\eta)}{p_0} + (\gamma - 1) M_0^2 \frac{u_1(\eta)}{u_0} \right] \quad (41)$$

Equations (34), (36), (39), and (41) complete the first-order solution in terms of the parameter B_1 , the eigenvalue α , and the zeroth-order infinite wedge solution. The parameter B_1 is a scale parameter whose role in the solution will be clarified.

Interpretation of B_1 and α

To this point, neither equation (16) or (17) has been solved explicitly. Direct substitution of the solutions (34), (36), and (39) shows that when $\alpha \neq 0$, equations (16) and (17) are identically satisfied if and only if

$$B_1 C_1 = 0 \quad (42)$$

where C_1 is given by equation (38). Thus, either $B_1 = 0$, or

$$C_1 = \frac{\partial p_0}{\partial \beta} + \rho_0 u_0 \tan \lambda_0 \frac{\partial v_0}{\partial \beta} \frac{H(1)}{i C_0 G(1)} = 0 \quad (43)$$

The various possibilities are treated separately as follows:

(a) Supersonic flow, $M_0 > 1$. ($B_1 = 0$) - In the case of a supersonic shock layer, equation (43) cannot be satisfied. Recall that C_0 is pure imaginary for $M_0 > 1$, while the functions $H(1)$ and $G(1)$ are real.

Further,

$$\frac{H(1)}{i C_0 G(1)} = \frac{1}{|C_0|} \frac{(1 + |C_0|)^\alpha + (1 - |C_0|)^\alpha}{(1 + |C_0|)^\alpha - (1 - |C_0|)^\alpha} \quad (44)$$

It can be readily shown from the oblique shock relations that

$$C_0 = \sqrt{M_0^2 - 1} \tan \lambda_0 < 1 \quad (45)$$

and thus

$$\frac{H(1)}{iC_0 G(1)} > 1 \quad (46)$$

If equation (38) is divided by the product $\rho_\infty V_\infty^2$ (ρ_∞ and V_∞ are the undisturbed stream density and velocity), and the oblique shock relations are applied, then

$$\frac{C_1}{\rho_\infty V_\infty^2} = \frac{4}{\gamma + 1} \sin \beta_0 \cos \beta_0 \left[1 - \frac{H(1)}{iC_0 G(1)} \right] - \frac{\sin \theta \cos \theta}{\cos^2 \lambda_0} \frac{H(1)}{iC_0 G(1)}$$

← which is strictly negative by virtue of equation (46). The conclusion from equation (42) is thus $B_1 = 0$ for $M_0 > 1$, with the further result that the first-order functions f_1 are all identically zero. The interpretation of this result is that the zeroth-order infinite-wedge solution prevails throughout the flow to at least a value ξ where the wedge contour departs from its original straight line. This feature is, of course, well known from other considerations, such as the hyperbolic character of the full equations for $M_0 > 1$. That is, there is no "feedback" of downstream disturbances in a locally supersonic flow.

(b) Subsonic flow, $M_0 < 1$. ($C_1 = 0$) - In the subsonic case, both physical reasoning and the elliptic nature of the full equations for $M_0 < 1$ suggest that the first-order solution is nontrivial. In fact, α is the eigenvalue which is determined by the requirement that C_1 vanishes, equation (43). When $M_0 < 1$, C_0 is real, and equations (31) and (32) are used. Hence,

$$\frac{H(1)}{iC_0 G(1)} = -\frac{1}{C_0} \cot \alpha \phi(C_0) \quad (47)$$

where

$$\phi(C_0) = \tan^{-1} C_0 \quad (48)$$

If nontrivial solutions for the first-order functions are to be obtained, that is $B_1 \neq 0$, then comparison of equations (43) and (47) shows that α must satisfy

$$\alpha = \tan^{-1} \left[\frac{\rho_0 v_0 \tan \lambda_0 \frac{\partial v_0}{\partial \beta}}{C_0 \frac{\partial p_0}{\partial \beta}} \right] / \tan^{-1} C_0 \quad (49)$$

When the oblique shock expressions are again inserted, equation (49) can also be written as

$$\alpha = \tan^{-1} \left[\left(1 - \frac{\gamma + 1}{4} \frac{\sin 2\theta}{\sin 2\beta_0 \cos^2 \lambda_0} \right) / C_0 \right] / \tan^{-1} C_0 \quad (50)$$

Examination of equations (49) and (50) reveals the following: In the subsonic interval, as the wedge angle increases from θ_s to θ_d , α decreases from $+\infty$ to 0. For $\theta_c < \theta \leq \theta_c$, $\infty > \alpha \geq 1$; for $\theta_c < \theta \leq \theta_d$, $1 > \alpha \geq 0$. These features can be observed by noting:

(1) As $C_0 \rightarrow 0$, $\alpha \rightarrow \infty$

(2) At Crocco's point, the streamline curvature behind a curved shock wave changes sign. It can be shown (see eq. (4-39), page 683 of Ferri, 1954, and also eq. (C-15), Appendix C of South, 1964) in terms of the present notation that the following relation holds:

$$C_0^2 \frac{\partial p_0}{\partial \beta} = \rho_0 u_0 \tan \lambda_0 \frac{\partial v_0}{\partial \beta} \quad (51)$$

and thus $\alpha = 1$.

(3) When $\alpha = 0$, an equation is obtained which relates the detachment wedge angle θ_d , the corresponding shock wave angle β_d , and γ , independent of the stream Mach number. That is, from equation (50)

$$1 - \frac{\gamma + 1}{4} \frac{\sin 2\theta_d}{\sin 2\beta_d \cos^2 \lambda_d} = 0 \quad (52)$$

Further manipulation yields a quadratic equation in $\tan \theta_d$, thus

$$\tan \theta_d = \frac{a}{b} \left[1 - b \pm \sqrt{1 - 2b} \right] \quad (53)$$

where

$$\left. \begin{aligned} a &= \cot \beta_d \\ b &= \frac{2}{\gamma + 1} (\sin 2\beta_d)^2 \end{aligned} \right\} \quad (54)$$

Most tables and charts for the oblique shock relations (e.g., Ames, 1953, pp. 42-43) exhibit a curve which separates the "strong shock" solution from the "weak shock" solution. Equation (53) is the equation of that curve in the β, θ plane, which is sometimes referred to as the detachment curve. (The author is not aware if equation (53) has been previously reported.) That it is, in fact, the detachment curve is clear in the present analysis since the solution breaks down for $\alpha = 0$, and an attached shock wave is no longer possible.

The parameter B_1 cannot be determined when $M_0 < 1$. The full equations are of elliptic type in this case, and the problem is under-specified by one boundary condition. The local solution cannot, of course, be extended arbitrarily far downstream, thus B_1 remains as a free scale parameter. It should be noted that for $\alpha = 1$ only, $d\beta(0)/d\xi$ is finite and different from zero, and B_1 is thus proportional to the shock-wave curvature at the vertex.

(c) Sonic flow, $M_0 = 1$. - The sonic condition, $M_0 = 1$, is the dividing point between the elliptic and hyperbolic character of the full equations and their required boundary conditions. Essentially the same

results are obtained whether the condition is approached from the subsonic range or the supersonic range. That is, in the subsonic-to-sonic approach, $\alpha \rightarrow \infty$; while in the supersonic-to-sonic approach, $B_1 = 0$. Both results state that in a neighborhood of the vertex of a finite sonic wedge, the infinite wedge solution is unaltered.

Pressure behavior near the vertex

In an experimental investigation of supersonic flow over a wedge, the surface pressures and shockwave shape can be measured directly. However, obvious physical restrictions prevent the placement of a pressure tap at the vertex. It is of particular interest, then, to understand the behavior of the surface pressure in a neighborhood of the vertex, as given by equation (36). In the range of wedge angles $\theta_s < \theta < \theta_d$, it has been shown that equation (43) holds; that is, $C_1 = 0$, and thus

$$p_1(0) = -\rho_0 u_0 \tan \lambda_0 \frac{\partial v_0}{\partial \beta} \frac{H(0)}{10G(1)} B_1 \quad (55)$$

A convenient parameter is suggested which represents the departure of the surface pressure from its value at the vertex, in terms of x ,

$$\mathcal{P} = \frac{p(x,0) - p(0,0)}{B_1 \rho_\infty V_\infty^2} \sim \frac{p_1(0)}{B_1 \rho_\infty V_\infty^2} x^\alpha \quad (56)$$

The computational form for ϕ is obtained by using equations (31), (55), and (56) to yield

$$\phi \sim \frac{\rho_0 u_0}{\rho_\infty V_\infty^2} \tan \lambda_0 \frac{\partial \gamma_0}{\partial \beta} \left[c_0 (1 + c_0^2)^{\alpha/2} \sin \alpha \phi(c_0) \right]^{-1} x^\alpha \quad (57)$$

Figure 3 and the companion table illustrate a worked example for $\gamma = 1.4$ and $M_\infty = 2$. For a wedge which terminates with a sharp corner or a gradual turn away from the free stream, the subsonic flow near the vertex will accelerate to sonic speed at or near the "shoulder," and the shock wave will be generally convex facing the stream. That is, B_1 will be negative, and hence positive values of ϕ indicate an acceleration of the flow with a corresponding decrease in pressure. The changing character of the flow is clearly evident as the wedge angle θ increases from θ_s to θ_d . For $\theta_s < \theta < \theta_c$, the pressure decrease is gradual; but for $\theta_c < \theta < \theta_d$, the pressure gradient is infinite.

Although in the present calculations the scale is unknown, it is intuitively obvious that the magnitude of B_1 will vary inversely as the physical size of the finite wedge such as the distance of the sonic shoulder from the vertex. If x^* is that distance, then $B_1 \rightarrow 0$ as $x^* \rightarrow \infty$, and the infinite-wedge solution is extended indefinitely.

3. CONCLUDING REMARKS

It has been shown that the analysis of the flow behavior during transition to shock detachment for a wedge is straightforward in the

transformed physical plane. In fact, the results for the first-order solution are complete and quantitative up to the undetermined scale parameter, B_1 .

The consideration of the effects of a nonzero surface curvature at the vertex is beyond the scope of the present paper, but should present no real difficulty. One expects the surface curvature to dominate the flow behavior for $\theta < \theta_c$, since the curvature terms will be linear in ξ . For $\theta_c < \theta < \theta_d$, however, the strong singularities (infinite gradients) observed in this range will prevail.

It was mentioned in the introduction that the basic approach presented here is adaptable to axisymmetric conical flow. More generally, it is applicable to pointed bodies of revolution with a well-defined surface normal. The body-oriented coordinate system and the subsequent transformation of the shock layer to an open rectangular region is ideally suited for such studies. The great advantage is the ease of application of the boundary conditions at the shock wave ($\eta = 1$) and at the body ($\eta = 0$). In other coordinates, such as spherical-polar, certain difficulties arise in this regard which can lead to spurious singularities in the higher-ordered solutions. Van Dyke (1954) has discussed this feature in regard to the work of Shen & Lin.

The extension of the present analysis to the circular cone is straightforward with the inclusion of the radius normal to the cone axis in equation (1). The coefficients of the analogous system for the first-order solution, equations (16)^{to} (18), will contain the zeroth-order

nonconstant, infinite-cone solution, which is known only by prior numerical solution. The determination of the eigenvalue α in the range of cone angles* $\theta_s < \theta < \theta_2$ would thus require a cut-and-dry^t numerical integration procedure; that is, the integration would start at the shock wave, $\eta = 1$, with repeated choices of α until the boundary condition $v_1(0) = 0$ is satisfied. Special attention to the nature of the solution near $\eta = 0$ will be necessary, as a singular behavior is expected there (Van Dyke, 1954). The linearity of the first-order equations and boundary conditions will allow the absorption of the unknown scale parameter B_1 .

*Here θ_s is the cone vertex angle for which the flow at the surface first becomes sonic; at $\theta = \theta_s$, the flow near the shock is still slightly supersonic.

REFERENCES

- Ames Research Staff 1953 Equations, tables, and charts for compressible flow. N.A.C.A. Technical Report 1135.
- Cabannes, H. 1951 Etude de l'onde de choc attachée dans les écoulements de révolution. Rech. aéro. 24, 17-23.
- Crocco, L. 1937 ⁿ Singolarità della corrente gassosa iperacustica nell'intorno di una prora a diedro. L'Aerotechnica 17, 519-34.
- Ferri, Antonio 1954 Supersonic flows with shock waves. General Theory of High Speed Aerodynamics. High Speed Aerodynamics and Jet Propulsion. VI, sec. H, W.R. Sears, ed., Princeton Univ. Press, 670-747.
- Guderley, K. Gottfried 1947 Considerations of the structure of mixed subsonic-supersonic flow patterns. Wright Field Rep. F-TR-2160-ND.
- Kopal, Zdenek 1947 Tables of supersonic flow around cones. Mass. Inst. of Technology Tech. Rep. 1.
- Shen, S. F. & Lin, C. C. 1951 On the attached curved shock in front of a sharp-nosed axially symmetrical body placed in a uniform stream. N.A.C.A. Technical Note 2505.
- South, Jerry O., Jr. 1964 Application of the method of integral relations to supersonic nonequilibrium flow past wedges and cones. N.A.S.A. Technical Report R-205.
- Van Dyke, Milton D. 1954 A study of hypersonic small-disturbance theory. N.A.C.A. Technical Report 1194.

Captions for Figures

Figure 1. Geometry and coordinates

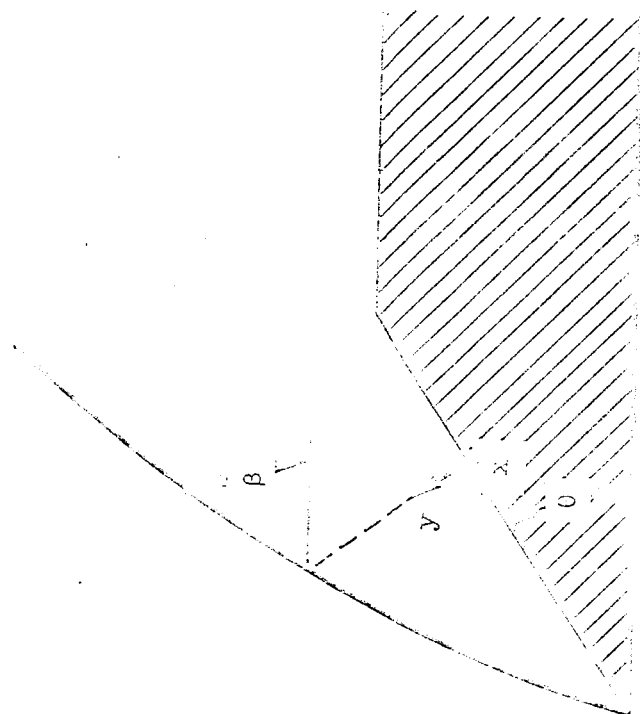
Figure 2. Transformed physical plane

Figure 3. Tip-pressure gradient parameter \mathcal{P} vs x . (See table for data.)
 $\gamma = 1.4$, $M_\infty = 2$

Table for Figure 3

Curve no.	θ	β	α	\mathcal{P}/x^α
*1	22.706°	61.485°	∞	∞
2	22.767	61.880	8.1078	1.0711
3	22.820	62.275	4.1922	.8283
4	22.866	62.670	2.5424	.7365
5	22.904	63.064	1.6072	.6910
**6	22.934	63.459	1.0000	.6662
7	22.948	63.701	.7223	.6570
8	22.959	63.943	.4985 ³⁶	.6509
9	22.967	64.185	.3021	.6470
10	22.972	64.427	.1395	.6450
*11	22.974	64.669	0 →	.6445

*Sonic; $\mathcal{P} \equiv 0$ for $0 \leq x < 1$
 ** Crocco's point
 *Detachment



$\rho_{\infty}, V_{\infty}, M_{\infty}$

Figure 1

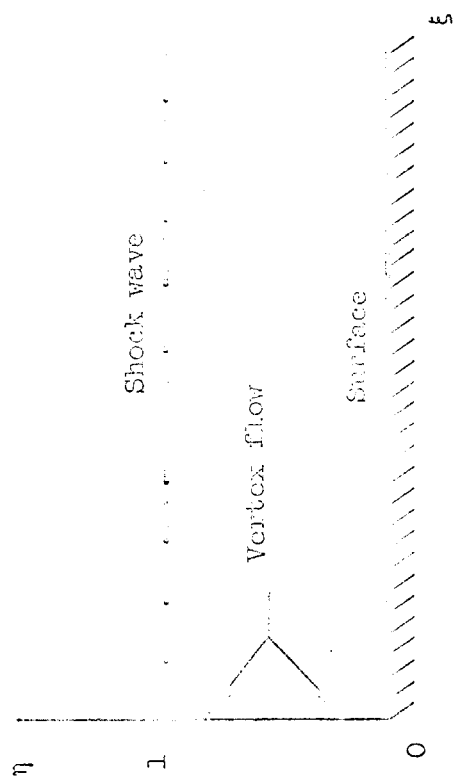


Figure 2

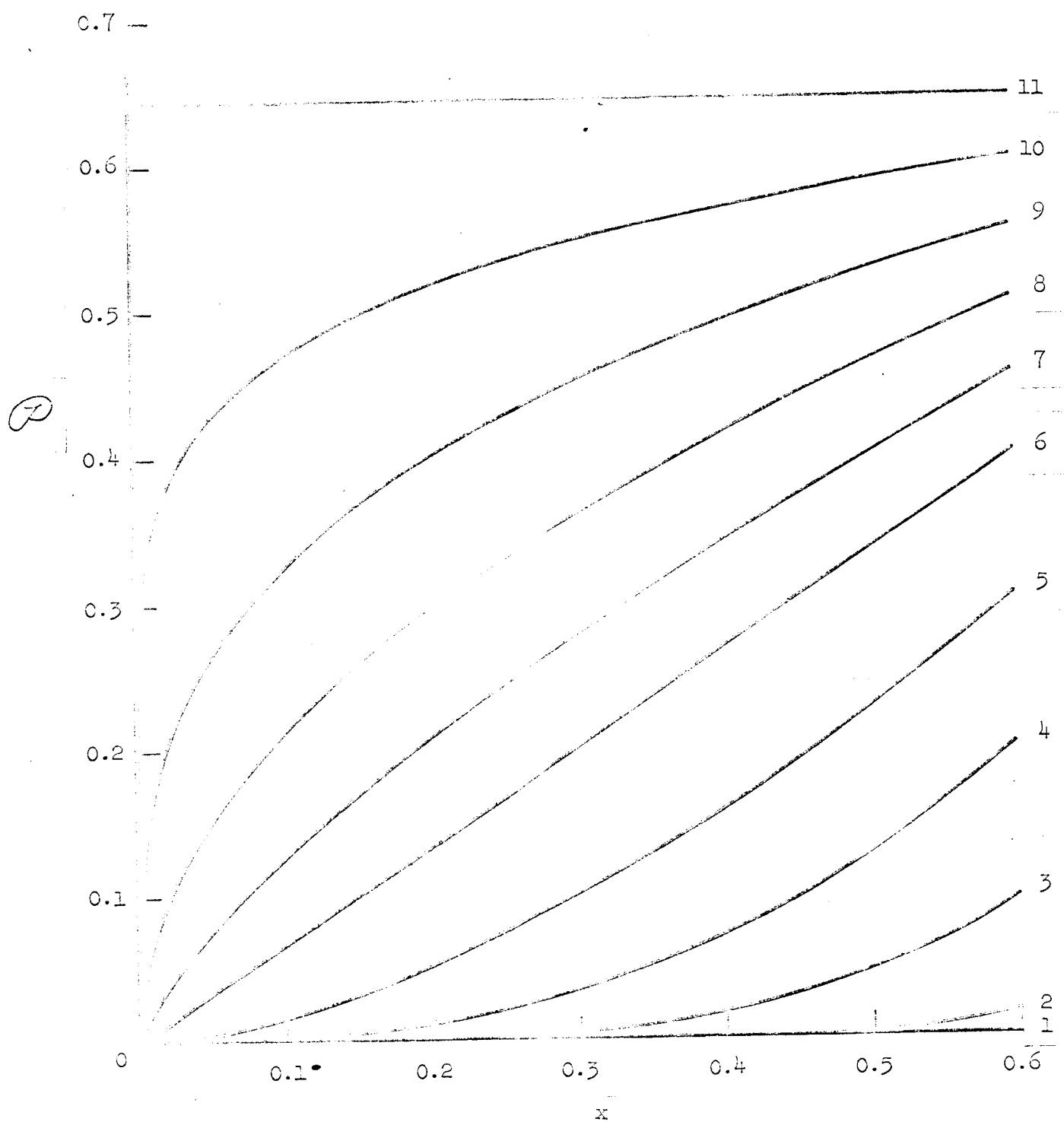


Figure 3